



## Material Image Segmentation with the Machine Learning Method and Complex Network Method

Chuanbin Lai<sup>1</sup>, Leilei Song<sup>1</sup>, Yuexing Han<sup>2,1,\*</sup>, Qian Li<sup>3</sup>, Hui Gu<sup>3</sup>, Bing Wang<sup>1</sup>, Quan Qian<sup>1,2</sup>  
and Wei Chen<sup>4</sup>

<sup>1</sup>School of Computer Engineering and Science, Shanghai University, 99 Shangda Road, Shanghai, CHINA, 200444;

<sup>2</sup>Shanghai Institute for Advanced Communication and Data Science, Shanghai University, 99 Shangda Road, Shanghai, CHINA, 200444;

<sup>3</sup>Material Genome Institute & School of Materials Science and Engineering, Shanghai University, 99 Shangda Road, Shanghai, CHINA, 200444;

<sup>4</sup>Key Laboratory of Power Beam Processing, AVIC Manufacturing Technology Institute, Beijing, CHINA, 100024;

\* hanyuexing@gmail.com

### Abstract

*The study of the relationship among the manufacturing process, the structure and the property of materials can help to develop the new materials. The material images contain the microstructures of materials, therefore, the quantitative analysis for the material images is the important means to study the characteristics of material structures. Generally, the quantitative analysis for the material microstructures is based on the exact segmentation of the materials images. However, most material microstructures are shown with various shapes and complex textures in images, and they seriously hinder the exact segmentation of the component elements. In this research, machine learning method and complex networks method are adopted to the challenge of automatic material image segmentation. Two segmentation tasks are completed: on the one hand, the images of the titanium alloy are segmented based on the pixel-level classification through feature extraction and machine learning algorithm; on the other hand, the ceramic images are segmented with the complex*

networks theory. In the first task, texture and shape features near each pixel in titanium alloy image are calculated, such as Gabor filters, Hu moments and GLCM (Gray-Level Co-occurrence Matrix) etc.. The feature vector for the pixel can be obtained by arraying these features. Then, classification is performed with the random forest model. Once each pixel is classified, the image segmentation is completed. In the second task, a complex network structure is built for the ceramic image. Then, a clustering algorithm of complex network is used to obtain network connection area. Finally, the clustered network structure is mapped back to the image and getting the contours among the component elements. The experimental results demonstrate that these methods can accurately segment material images.

## INTRODUCTION

Most of material images contain complicated textures and microstructures with various shapes. As shown in Figure 1, (a) is images of the titanium alloy TiAl, which include two kinds of phases in the TiAl images: the stripe phase marked in rectangle, and the block phase marked in ellipse. To calculate the ratio and distribution characteristics of the two phases, the segmentation of the two phases is a primary task. Since there is no obvious boundary between the two phases and the textures in the images are very complicated, it is a difficult task to distinguish the two phases. Another kinds of image is the multiphase ceramic TiB<sub>2</sub>-TiC shown in Figure 1 (b), the image can roughly be divided into five categories according to grayscale value: white, shallow-gray, gray, dark-gray and black. The five categories correspond to the WC impurity gather zone, the rich TiC phase zone, the normal multi-phase zone, the rich TiB<sub>2</sub> phase zone as well as the holes and non-dense zone. As shown in Figure 1 (b), different color blocks are embedded with each other, and the boundaries between different phases are even more obscure, such as the region circled by the black curve.

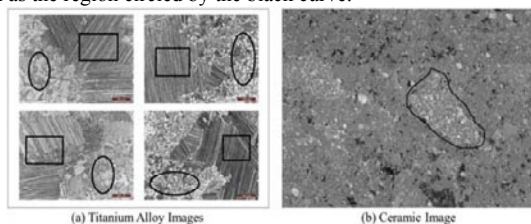


Figure 1: The material images. (a) are images of the titanium alloy TiAl. (b) is an image of the ceramic TiB<sub>2</sub>-TiC.

There have been some methods related to the segmentation of the material images. Chen et al. [1] and Liu et al. [2] both improved the traditional Watershed method to solve the over-segmentation problem in the segmentation of the metallographic images. The two methods are based on traditional image processing techniques, and they are only suitable for segmenting images with obvious boundaries. Albuquerque et al. [3] and He et al. [4] applied the artificial neuronal network in the segmentation and quantification of microstructures in the images. However, these methods only use simple image features, such as the pixel value. Thus, they are hard to accurately segment images which have complicated textures. Azimi et al. [5] proposed a segmentation method based on Fully Convolutional Neural Networks (FCNN) [6] for microstructural classification in the images of low carbon steel. This method can obtain good results, while the training of the model needs a larger number of samples. Since the images of some kind of material are scarce, the application of deep learning in material images segmentation is limited.

In order to effectively segment the material images with obscure boundaries, we propose two methods for two different conditions. For the segmentation of material images which have a certain number of samples, the machine learning method is utilized. For the segmentation of material images which have very unclear boundaries, the complex networks method is adopted. The experimental results show that our approaches have high segmentation precision.

## APPROACHES

### Segmentation with Machine Learning Method

#### *Feature extraction*

Feature extraction is the first step in the machine learning based segmentation method. To represent the characteristics of the rich and complex textures in materials image, four feature extraction methods are applied and introduced as follows.

The Gabor filter [7, 8] is a linear filter used for texture analysis. Frequency and orientation representations of the 2D Gabor filters are similar to the representations of the human visual system. Therefore, the 2D Gabor filter is appropriate for texture representation and discrimination. In our method, six orientations  $[0^{\circ}, 30^{\circ}, 60^{\circ}, 90^{\circ}, 120^{\circ}, 150^{\circ}]$  are used to generate six Gabor filters with different orientations. The size of the Gabor filter is  $l \times l$ . The six Gabor filters are convolved with the original image to obtain six feature maps. Hence, for each pixel, 6 dimensional feature vectors can be obtained from the six feature maps.

Hu moment [9] is a kind of shape-based feature descriptors which has translation-invariance, rotation-invariance and scale-invariance. Hu moment consists of seven moment invariants. In our approach, the  $l \times l$  ROIs centered on each pixel are extracted to compute the Hu moment. Therefore, a 7-dimensional feature vector is got for each pixel through the Hu moment method.

Histogram of oriented gradients (HOG) [10] describes a set of histograms of gradient orientations for an image. The HoG can reflect the distribution characteristics of intensity gradients and edge directions in an image. Here, the HoG of each ROI are calculated as one of the features of the pixels. The size of the ROI is also  $l \times l$ . The number of bins in the histogram is set to 9 in our method. Each bin in a histogram records the number of times a gradient orientation occurs in a ROI. With HoG method, a 9-dimensional feature vector can be calculated for each pixel.

Gray-level co-occurrence matrix (GLCM) [11] is a matrix which records the distribution of co-occurring pixel pairs at some certain conditions. The GLCM can measure the characteristics of image texture in orientation, distance and transformation. In our approach, the GLCM  $G_{\epsilon-\alpha}$  is calculated for the  $l \times l$  ROI centered on each pixel. The  $\epsilon$  and  $\alpha$  are the distance and orientation between the pixel pairs, respectively. In our method, the  $\epsilon$  is set to 2. Four direction  $(0^{\circ}, 45^{\circ}, 90^{\circ}, 135^{\circ})$  are chosen to calculate four GLCMs  $\{G_{2-0^{\circ}}, G_{2-45^{\circ}}, G_{2-90^{\circ}}, G_{2-135^{\circ}}\}$  for a ROI. As introduced in the study which was conducted by Haralick et al. [20], features can be generated from the  $G_{\epsilon-\alpha}$ . Four features are applied in our method, i.e., the contrast  $Con_{\epsilon-\alpha}$ , the angular second moment  $Asm_{\epsilon-\alpha}$ , the entropy  $Ent_{\epsilon-\alpha}$  and the correlation  $Corr_{\epsilon-\alpha}$ . Thus, four GLCMs are calculated in four orientations for a ROI. Then, four features  $(Con_{\epsilon-\alpha}, Asm_{\epsilon-\alpha}, Ent_{\epsilon-\alpha}, Corr_{\epsilon-\alpha})$  can be derived from each matrix  $G_{\epsilon-\alpha}$ . In other word,  $4 \times 4$  features are extracted for each pixel with the GLCM method. To reduce the dimension of the feature, the variances of the four features in four orientations are calculated, respectively, i.e.,  $(Var_{Con}, Var_{Asm},$

$\text{Var}_{\text{Ent}}$ ,  $\text{Var}_{\text{Corr}}$ ). As a result, the 4-dimensional feature vectors are extracted for each pixel by using the GLCM method.

### *Classification and segmentation*

As mentioned in the Section 2.1.1, each pixel can be represented by a concatenated 26 dimensional feature vector. The following step is classifying the pixels with a classifier. In this paper, the random forest (RF) [12] algorithm is applied to train the classifier. The RF algorithm is an ensemble learning method which is comprised of multiple decision trees. A decision tree is a classification model which has the tree structures. The algorithms for constructing decision trees usually work top-down by choosing a feature which best splits the set of data at each step. Here, the CART algorithm [13] is applied to construct each decision tree.

The decision trees tend to grow very deep and overfit the training sets. The Random Forest is a way to alleviate the overfitting problem by using multiple simple decision trees. Each decision tree is trained on a random subset of the dataset and a random subset of the features, and the depth of the tree is limited. In the classification, each tree gives a class label, and the random forest chooses the class label with the most votes as the final class. Once each pixel is classified, the image segmentation is achieved.

### Segmentation with Complex Network Method

The complex network method is based on graph theory and statistical mechanics. This method consists of three major parts for segmenting the material images with unclear boundaries. The first part mainly includes the extraction of the segmented object pixels and definition of a set of nodes. Then, the nodes are divided into unit grids [14], and a set of nodes are defined based on the number of pixel in each grid. In the second part, the similarity [15] between nodes is calculated based on the node coordinate information. Each node is mapped into a vertex of the complex network. Subsequently, the basic network topology is built by connecting each node pair by using a threshold radius. For vertexes in the network topology, two vertexes are connected only if the similarity between them is lesser than a radius and its density is higher than a given density threshold. Finally, the contours extracting algorithm [16] is applied to obtain each segmented region contours, and the contours are mapped to the original material image according to the network topology.

## **EXPERIMENTAL RESULTS AND DISCUSSION**

### Experimental Results with Machine Learning Method

In order to evaluate the performance of the machine learning method in the segmentation task, 12 alloy TiAl images are used to test the method. The 12 images are randomly divided into 6 groups, and each group contains 2 images. Then, 6-fold cross validation is performed on the 6 groups of images. The parameter  $l$  in feature extraction is set to 5 in the experiments. The precision, recall and F-score are used as quantitative performance evaluation. The quantitative evaluation of the machine learning method is illustrated in Table 1. Figure 2 shows the segmentation results.

From the Table 1, the average precision, recall and F-score are all more than 0.85. The worst performance appears in validation 2, and the best performance appears in validation 1. Through the Row (1) and (2) in Figure 2, which are the results of validation 2, the error mainly comes from the regions which have wide and sparse stripes as marked

in ellipse. This is mainly because the characteristics of the wide stripe-regions and the block-regions are similar and difficult to distinguish. In contrast, the segmentation of the images with slim and dense stripes is able to achieve high performance, as shown in the Row (3) and (4) Figure 2, which are the results of validation 1.

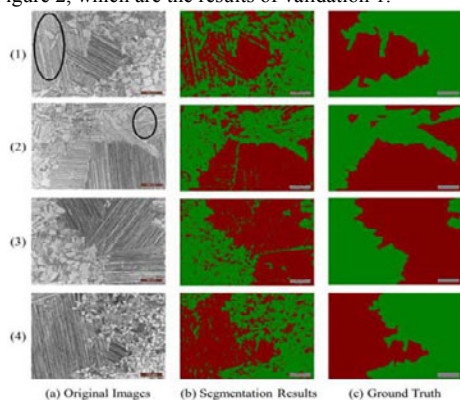


Figure 2: Segmentation results. Column (a) is original images. Column (b) is the segmentation results with machine learning method. Column (c) is the ground truth marked manually.

Table 1: The quantitative evaluation of the machine learning method

Validations	Precision	Recall	F-score
validation 1	0.901	0.909	0.905
validation 2	0.771	0.784	0.777
validation 3	0.850	0.882	0.866
validation 4	0.879	0.898	0.888
validation 5	0.855	0.891	0.873
validation 6	0.862	0.869	0.865
Mean	0.853	0.872	0.862

### Experimental Results with Complex Network Method

In this experiment, a microscopic image of  $TiB_2-TiC$  multiphase ceramics is used as the experimental material, as shown in figure 3 (a). There is no obvious boundary between the phase zones. The method of complex network is applied to achieve the segmentation of dense  $TiC$  phase zone. The segmentation result is shown in Figure 3 (b).

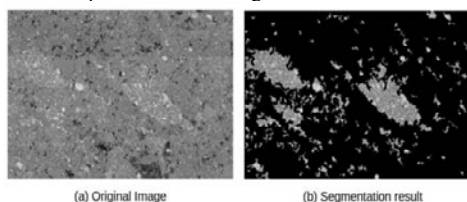


Figure 3: The segmentation result with the complex network. (a) original images. (b) the segmentation result.

## CONCLUSION

In this work, the machine learning method and the complex network method are proposed to segment the material images. The experiments demonstrate that the images can be accurately segmented by the two methods. Thus, the proposed methods provide a reliable technical support to effectively segment the material images.

## Acknowledgments

This research is sponsored by Shanghai Pujiang Program (17PJ1402900), the National Key Research and Development Program of China(No.2018YFB0704400, No.2018YFB0704402), the National Science Foundation for Young Scientists of China (Grant No. 61603237), the Program for Professor of Special Appointment (Eastern Scholar) at Shanghai Institutions of Higher Learning, the National Natural Science Foundation (Grant No. 51532006) and Aeronautical Science Fund "Integrated computational research of the additive manufacturing for ultra-high strength Ti alloys" (2017ZF25022).

## References

1. Chen Y, Chen J. A watershed segmentation algorithm based on ridge detection and rapid region merging. in: Signal Processing, Communications and Computing (ICSPCC), 2014 IEEE International Conference on, IEEE, 2014:420-424.
2. Liu J, Chen J. An improved iterative watershed according to ridge detection for segmentation of metallographic image. *Metallographic Image*, 2012:8.
3. Albuquerque D, Victor H C, Jo'o Manuel R S, Cortez P C. Quantification of the microstructures of hypoeutectic white cast iron using mathematical morphology and an artificial neural network. *Inter-national Journal of Microstructure and Materials Properties*, 2010, 5(1):52-64.
4. He W N, Zhang L L. Study on artificial neuronal networks applied on microstructure segmentation from metallographic images. *Electronic Design Engineering*, 2013, 3:49.
5. Azimi S M, Britz D, Engstler M, Fritz M, Mucklich F. Advanced Steel Microstructural Classification by Deep Learning Methods, *Scientific reports*, 2018, 8(1).
6. Long, J., Shelhamer, E. & Darrel, T. Fully convolutional networks for semantic segmentation. In *IEEE Conference on Computer Vision and Pattern Recognition (CVPR)* (2015).
7. Feichtinger H G, Luef F. Gabor Analysis and Algorithms[J]. *Applied & Numerical Harmonic Analysis*, 1998, 1:123-170.
8. Feichtinger H G, Thomas Strohmmer Eds. *Gabor analysis and algorithms: Theory and applications*. Springer Science & Business Media, 2012.
9. Hu, M K. Visual pattern recognition by moment invariants. *IRE transactions on information theory*, 1962, 8(2): 179-187.
10. Dalal N, Bill T. Histograms of oriented gradients for human detection. *Computer Vision and Pattern Recognition*, 2005. *CVPR 2005. IEEE Computer Society Conference on*, 2005:1.
11. Haralick R M, Karthikeyan S. Textural features for image classification. *IEEE Transactions on systems, man, and cybernetics*, 1973, 6: 610-621.
12. Breiman, L. Random forests. *Machine learning*, 2001, 4(1): 5-32.
13. Breiman L, Friedman J H, Olshen R A, Stone C J. *Classification and regression trees*. 1984.
14. Cuadros O, Botelho G, Rodrigues F, Neto JB. Segmentation of large images with complex networks. *SIBGRAPI 2012: 24-31*. DOI: 10.1109/SIBGRAPI.2012.13.
15. B. B. Machado, L. F. Scabini, J. P. M. Orue, M. S. de Arruda, D. N. Goncalves, W. N. Goncalves, R. Moreira, and J. F. Rodrigues-Jr, A complex network approach for nanoparticle agglomeration analysis in nanoscale images, *Journal of Nanoparticle Research*, 2017, 19(2):65.
16. Suzuki S. and Abe K: Topological structural analysis of digital binary images by border following, *CVGIP*, 1985, 30:52-46.